Journal of Alloys and Compounds 520 (2012) 93–97

Contents lists available at SciVerse ScienceDirect

Journal of Alloys and Compounds

journal homepage: www.elsevier.com/locate/jallcom

High-pressure elasticity and lattice dynamics of Mg_2La from first principles

Savaş Ağduk, Gökhan Gökoğlu*

Department of Physics, Karabük University, 78050 Karabük, Turkey

ARTICLE INFO

Article history:
Received 10 October 2011
Received in revised form
22 December 2011
Accepted 23 December 2011
Available online 2 January 2012

Keywords:
Intermetallics
Elasticity
Phonons
Computer simulations

ABSTRACT

In this study, we present the results of first principles calculations of elastic constants and structural properties of the Mg_2La cubic Laves phase (C15) up to ≈150 GPa pressure together with vibrational properties at equilibrium geometry. projector augmented wave (PAW) potentials are used with generalized gradient approximation (GGA) scheme of the density functional theory. The linear response technique of the density functional perturbation theory is applied in investigation of the phonon dispersion spectra. The static equation of states of the system has been studied with Vinet formulation. The values of applied pressure have also been obtained from the Vinet formulation of equation of states. The cubic phase of the system remains stable within the studied pressure range. The elastic anisotropy ratio indicates an electronic topological transition (ETT) around ≈100 GPa. This situation is also confirmed by electronic band structures.

1. Introduction

Magnesium based pseudo-binary alloy systems with a general formula $Mg_2(RE)$ (RE: rare-earth element) have been taking place at the center of several theoretical [1,2] and experimental [3] studies due to the interesting electronic and mechanical properties. Magnesium alloys are exceedingly important with applications in the automobile and aircraft industry [1]. The utilization of magnesium alloys in automobile industry has a growing trend indicating 15% annual increase over the last decade [4,5]. These compounds can be stabilized in hexagonal C14 ($MgZn_2$ type) and C36 ($MgNi_2$ type), and cubic C15 ($MgCu_2$ type) structures according to the relation between the atomic radii of the constituent elements [6]. The only structural difference between cubic $MgCu_2$ and hexagonal $MgZn_2$ is the particular stacking of same four-layer structural units [7]. The close structural relationship between these types of phases has been first emphasized by Laves and Mitte [8], so these crystal structures are called "Laves phases". In a previous experimental study [9], it has been reported that (RE)Mg_2 compounds are able to form Laves phases.

The electronic structure of various Laves phases have been discussed and summarized in a recent review article [10]. The thermodynamic properties of several Mg–La binary alloy systems have been reported in a very recent comprehensive study using DFT scheme with GGA functionals [11]. There is a substantial progress in the high-temperature forming of Mg vehicle closure components [12]. This progress also leads to the implementation of Mg sheet alloys in vehicles. In another study, the solid-solution strengthening of magnesium has been studied from first principles [13]. In that work, the solubilities of several metals in magnesium have been computed using size and chemical misfits. The rare-earth addition to magnesium based Laves structures improves considerably the mechanical strength of the material [14] which is important particularly for technological applications. It was reported that the alloying abilities of MgLa, Mg_2La, and Mg_3La should be much stronger than the other known Mg–La systems such as $Mg_{17}La_2$ and $Mg_{12}La$ [15]. The recent works focus particularly on the formation enthalpies, zero pressure electronic and elastic properties [15–18] as well as high temperature thermodynamic properties of these systems [11]. In the work of Wróbel et al. [11], the phonon dispersion spectra have been computed for several Mg–La binary systems. However, the studies on mechanical properties and pressure-dependent elastic stiffness of these compounds are very rare. Naturally, the technological applications mentioned above involve the mechanical resistance of the material against pressure. The vibrational properties of C15 Laves structure of Mg_2La system have also been studied in the present study, since the microscopic mechanisms of elastic behavior is directly governed by the phonon properties. Therefore, the major aim of the present study is to clarify the pressure dependent elastic properties and vibrational dynamics of Mg_2La Laves phase using an accurate all-electron method, projector augmented wave, within density functional theory.

The rest of the paper is organized as follows: the details of calculations performed are presented in Section 2. We present the

* Corresponding author. Tel.: +90 370 433 8374; fax: +90 370 433 8334.
E-mail address: ggokoglu@gmail.com (G. Gökoğlu).

0925-8388/$ – see front matter © 2011 Elsevier B.V. All rights reserved.
doi:10.1016/j.jallcom.2011.12.131

results of the first-principles calculations of elastic constants at various pressures and phonon dispersion spectra in Section 3. Finally, a conclusion is presented in Section 4.

2. Computational method

The Mg_2La compound crystallizes in the face-centered cubic C15 Laves phase which conforms to $Fd\bar{3}m$ space group (#227) containing 6 atoms per primitive cell. La atoms are located on the site of diamond structure (8a positions), while Mg atoms occupy 16d positions. All the calculations presented in this study have been performed using the PWscf code, distributed with the Quantum ESPRESSO package [19,20].

Generalized gradient approximation of the density functional theory is used to approximate exchange-correlation potential with Perdew–Burke–Ernzerhof parametrization [21]. The ions are described using projector augmented waves (PAW) potentials. PAW is an all-electron method which generalizes the pseudopotential method and linear augmented plane wave (LAPW) method by taking into account the core electrons. In that sense, it presents an advantage over the usual pseudopotential method. We have produced the PAW potentials of Mg and La atoms using the ATOMPAW code developed by Holzwarth et al. [22]. In the generation of the lanthanum PAW data, a scalar relativistic scheme is followed. The non-linear core correction is applied to compensate the overlap of the core and valence charge densities giving an improved transferability. In order to generate smooth pseudo partial-waves, we use an eight-degree polynomial for lanthanum and RRKJ scheme [23] for magnesium as implemented in ATOMPAW code. The Vanderbilt procedure [24] is used as an orthogonalization scheme for projectors and partial-waves. The analytical form of the shape function is governed by the spherical Bessel functions [25]. Both of the PAW potentials produced by ourselves are now available at the pseudopotential database of the PWscf code [19]. The detailed convergence tests for these pseudopotentials are also included in the same database. As a preliminary remark, our PAW potentials converge to better than 0.1 meV per atom at a 70 Ry kinetic energy cut-off and $14 \times 14 \times 14$ k-point mesh in their respective crystal forms. We have computed the structural parameters of elemental solids of lanthanum and magnesium in order to prove the reliability of generated potentials. The calculated lattice parameters using these potentials are: $a = 3.76$ Å, $c/a = 3.220$ for alpha phase (hcp) of lanthanum and $a = 3.20$ Å, $c/a = 1.623$ for hcp structure of magnesium. These values are in great agreement with PBE and PBEsol calculations of Ref. [11].

In calculations on Laves structure, Brillouin zone integration is performed with automatically generated $14 \times 14 \times 14$ k-point mesh, following the convention of Monkhorst and Pack [26], yielding 104 k-points centered at Γ-point. Wave-functions are expanded in plane wave basis sets up to a kinetic energy cut-off value of 70 Ry. This produces approximately ≈11300 plane waves. The convergence criteria for total energy is 1×10^{-8} Ry in self-consistent calculations. Marzari–Vanderbilt type smearing is applied on fermionic occupation function with $\sigma = 0.02$ Ry smearing parameter [27].

The three independent elastic stiffness coefficients of the cubic crystal under study, C_{11}, C_{12}, and C_{44} are calculated using volume conserving (isochoric) strains. The use of isochoric strains eliminates the first order terms in energy due to the initial hydrostatic pressure. This procedure gives accurate results, since the energy of the crystal depends more strongly on volume than distortions [28]. The shear elastic constant C_s is calculated via tetragonal distortion, while a monoclinic distortion is used to calculate C_{44}. Under these distortions, the strain energies can be expressed as

$$E(\delta) = E(0) + 6C_s V\delta^2 + O(\delta^3), \quad (1)$$

$$E(\delta) = E(0) + 2C_{44} V\delta^2 + O(\delta^4) \quad (2)$$

for tetragonal (1) and monoclinic (2) distortions, respectively [29]. $E(0)$ is the unstrained ground state energy of the system and V is its volume. C_{44} and C_s are obtained from the quadratic coefficients of Eqs. (1) and (2). Other elastic constants (C_{11} and C_{12}) are calculated using C_s and bulk modulus B. The details of the elastic constant calculation method have been explained in detail in Refs. [30,31]. The hydrostatic pressure applied on the system has been realized by changing the lattice constant. The pressure value corresponding to a definite lattice constant is determined from pressure–volume curve of Vinet equation of states [32].

The full phonon dispersion spectra along the main symmetry directions in irreducible Brillouin zone are constructed by using DFPT in the linear response approach [33–35], in which second order derivatives of the total energy are calculated to obtain dynamical matrix. DFPT allows us to examine vibrational properties of materials at a high accuracy level. Energy threshold value for convergence is 1×10^{-16} Ry in phonon calculations. The dynamical matrices are produced in a k-point grid of $6 \times 6 \times 6$ in irreducible wedge of the Brillouin zone. Then the full phonon dispersion spectra can be calculated from interatomic force constants by Fourier transform of dynamical matrices.

3. Results and discussion

The formation of cubic C15 or hexagonal C14 Laves structures is realized according to the ratio of atomic radii of the constituent elements. For the X_2A stoichiometry, the cubic phase is formed if the following condition is satisfied;

$$\frac{d_A}{d_X} > \sqrt{\frac{3}{2}}$$

where d_A and d_X are the atomic radii of A and X atoms, respectively [6]. Otherwise, the hexagonal C14 phase is energetically favored. The atomic radii of Mg and La atoms are 1.50 Å and 1.95 Å [36], respectively, indicating an energetically favored cubic phase. It can be generalized that the formation of cubic phase is more probable for $Mg_2(RE)$ structures including a rare-earth element with less than half-filled 4f electronic orbital [3].

The structural parameters of the system (e.g., lattice constant and bulk modulus) have been studied by Vinet formulation [32] of equation of states (EOS) using energy vs. volume $E(V)$ variation which is obtained by calculation of total energies at more than 30 different volumes between the range 0.8 and 1.2 V_0, where V_0 is the equilibrium volume. The volume derivative of EOS formula gives pressure–volume $P(V)$ curve which is used to identify volume value corresponding to a given pressure. The asymptotic standard errors in EOS fit are less than 0.15% as an indication of the accuracy of performed calculations. In Fig. 1, the static equation of states of Mg_2La structure is shown as energy-lattice constant (a) and pressure–volume (b) variation. The calculated equilibrium volume is 168.819 Å^3 resulting 8.773 Å lattice constant. The calculated zero pressure bulk modulus is 36.71 GPa. The lattice constant of this C15 Laves phase was determined experimentally as 8.774 Å [37].

The second order elastic constants of the system are calculated using tetragonal and monoclinic distortions on face-centered cubic Laves structure as explained in previous section. The system is transformed into body-centered tetragonal structure under the isochoric tetragonal distortion, while a body-centered orthorhombic cell is created under the monoclinic distortion. Although the forces on the atoms are exactly zero in cubic phase, the ionic minimization is needed in order to optimize distorted structures. The minimization is performed using Broyden–Fletcher–Goldfarb–Shanno (BFGS) algorithm [38], until the forces on the atoms are less than

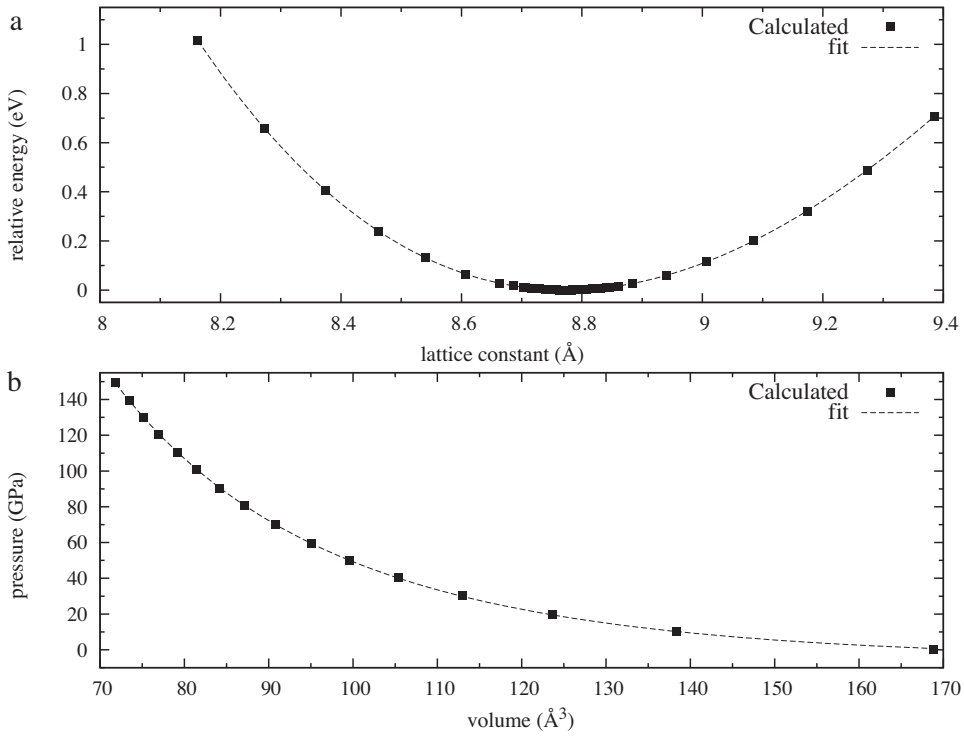

Fig. 1. Static equation of states of Mg_2La. (a) The total energies relative to equilibrium energy as a function of lattice constant and (b) pressure–volume curve within studied pressure range. Both are due to Vinet formulation.

1×10^{-4} Ry/a.u. Under this condition, the positions of the atoms are converged to less than 0.003 Å. We give the elastic constants of Mg_2La system at various pressures up to 150 GPa in Table 1. The shear elastic constant C_s and Voigt's shear modulus G_V can be expressed in terms of other elastic moduli as: $C_s = (C_{11} - C_{12})/2$ and $G_V = (2C_s + 3C_{44})/5$. The changes of elastic moduli as function of pressure are also shown in Fig. 2. In a previous theoretical study [17], the zero pressure elastic constants of this system were calculated as 58.4 GPa, 24.9 GPa, and 21.8 GPa for C_{11}, C_{12}, and C_{44}, respectively. These are in great agreement with the values presented in this work. The mechanical stability criteria for cubic crystals are: $(C_{11} - C_{12}) > 0$; $(C_{11} + 2C_{12}) > 0$; $C_{11} > 0$; $C_{44} > 0$, which are well satisfied within the studied pressure range indicating the stability of cubic phase.

The elastic anisotropy ratio is defined as $A = C_{44}/C_s$. This ratio is 1.490 at zero pressure and decreases to 0.982 at 100 GPa. As shown in the inset of Fig. 2, the A values reveal an interesting behavior with a minimum point around ≈100 GPa pressure which corresponds to the contraction of the lattice with a ratio of $V/V_0 = 0.48$. Since the cubic structure of the material remains stable within the studied pressure range, this behavior evokes an electronic topological transition (ETT) (also known as Lifshitz singularity [39,40]) which causes an anomaly in resistivity and thermoelectric power of the material, when the extremum of an energy band passes through Fermi level [41]. In Fig. 3, we display the three selected electronic bands which pass the Fermi level at Γ-point with increasing pressure. Fermi level of the system shifts to higher energies with increasing pressure as expected. But the shift of electronic bands are much larger than that of Fermi level resulting in a net upward movement of energy bands. Consequently, these bands become unoccupied at the upside of Fermi level. This anomaly in electronic structure can also be seen in pressure dependence of electronic

Table 1
Zero temperature static elastic constants of cubic C15 Mg_2La structure at various pressures. All elastic constants as well as pressure units are GPa. The elastic anisotropy ratio A is dimensionless.

Pressure	V(Å^3)	B	C_s	C_{11}	C_{12}	C_{44}	G	A
−0.010	168.819	36.71	14.82	56.47	26.83	22.08	19.18	1.490
10.406	138.356	70.33	25.76	104.67	53.16	31.19	29.01	1.211
19.914	123.661	96.72	34.72	143.01	73.57	38.61	37.05	1.112
30.321	112.940	122.86	43.35	180.66	93.96	47.10	45.60	1.086
40.421	105.347	146.27	50.37	213.43	112.69	54.71	52.97	1.086
50.097	99.642	167.34	55.94	241.93	130.04	60.28	58.54	1.077
59.426	95.113	186.66	60.15	266.86	146.56	64.10	62.52	1.066
70.143	90.743	207.92	64.41	293.80	164.98	66.81	65.85	1.037
80.482	87.156	227.60	68.40	318.79	182.00	69.05	68.79	1.010
90.465	84.144	245.93	72.34	342.38	197.70	71.59	71.89	0.990
100.862	81.390	264.31	76.94	366.90	213.02	75.54	76.10	0.982
110.309	79.157	280.50	81.22	388.80	226.36	79.87	80.41	0.983
120.621	76.965	297.63	86.34	412.75	240.07	86.11	86.20	0.997
129.946	75.170	312.65	91.03	434.02	251.97	92.04	91.63	1.011
139.436	73.490	327.59	96.28	455.97	263.41	98.94	97.88	1.028
149.631	71.836	343.22	101.91	479.09	275.28	106.80	104.84	1.048

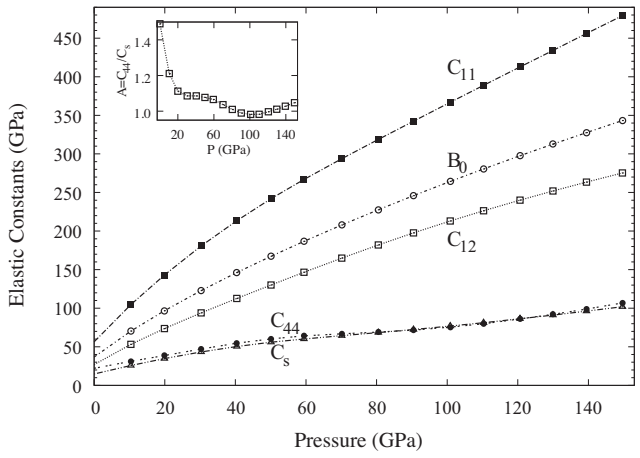

Fig. 2. Static elastic constants of C15 Mg_2La Laves phase as a function of pressure. The elastic anisotropy ratio is shown in the inset.

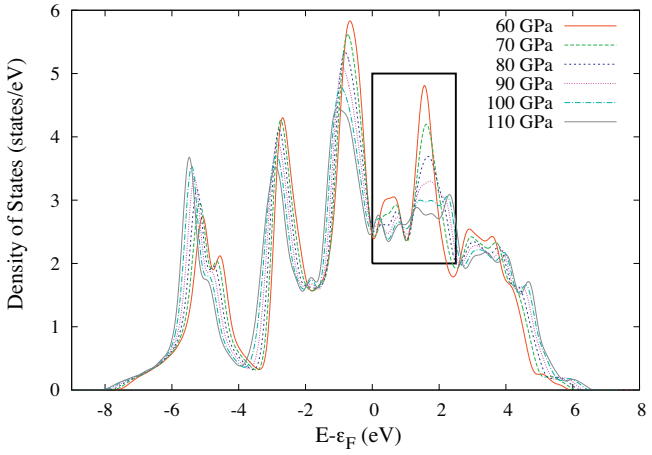

Fig. 4. Total electronic density of states of Mg_2La Laves phase between 60 and 110 GPa pressures.

density of states as given in Fig. 4. The two strong peaks which locate between 0 and 2 eV energy states are diminished due to the effects of pressure on electronic bands. This situation shows the importance of Fermi surface structure on elastic properties [29].

The ductility of a material can be determined according to its B/G ratio. According to Pugh [42], the plastic properties of metals can be linked empirically by their elastic behavior by B/G ratio. The materials having a B/G ratio greater than 1.75 are ductile, while materials having a B/G ratio less than 1.75 are brittle [2,17]. In previous studies, the ductile versus brittle transition in intermetallic compounds has been shown in view of the first principles calculations [43,44]. This ratio is 1.91 at zero pressure and increases monotonically with pressure as an indication of high ductility of cubic Mg_2La Laves phase. It can be stated that the material becomes more ductile under compression.

In Fig. 5, we display the zero pressure full phonon dispersion spectra of Mg_2La along the main symmetry directions in

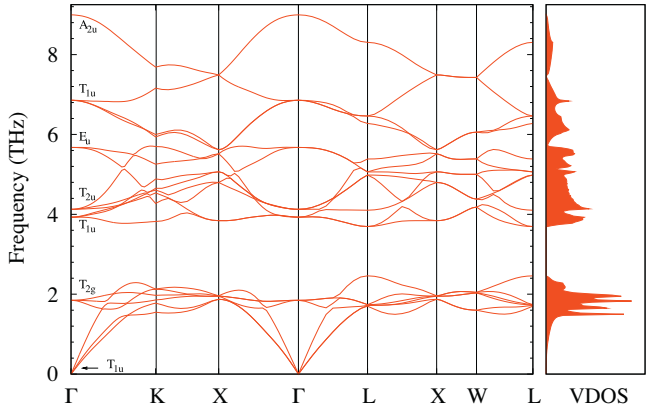

Fig. 5. The zero pressure ab initio phonon dispersion curves of C15 Mg_2La Laves phase together with total vibrational density of states.

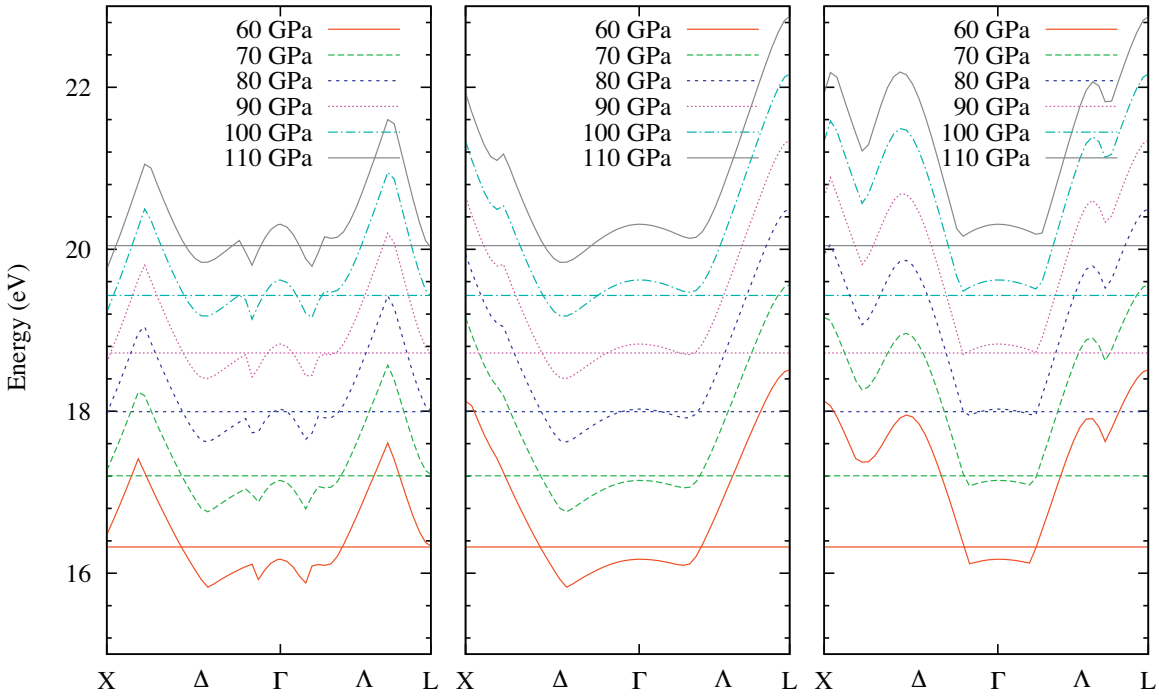

Fig. 3. The view of three selected electronic bands between the pressures 60 and 110 GPa with 10 GPa intervals. Fermi level of each band is associated with its color.

irreducible wedge of Brillouin zone. The symmetries of phonon modes at Γ-point are also shown in this figure. The overall spectra are in agreement with the recently reported first principles calculations of Wróbel et al. [11]. The vibrational spectra are composed of 3 acoustical and 15 optical modes resulting from 6 atoms per primitive cell. The transverse modes along Γ–X and Γ–L directions are doubly degenerate due to symmetry of the crystal, while the modes along Γ–K direction are non-degenerate. The large vibrational gap between ≈2.1 THz and ≈3.8 THz separates the acoustical and optical modes and is due to large atomic mass difference of magnesium and lanthanum atoms.

The expected IR and Raman peaks can be calculated from Group theory using crystal space symmetry and occupied Wyckoff crystallographic positions. There are seven irreducible presentation at zone center (Γ-point). The irreducible presentations corresponding to 15 optical modes are $3T_{2g} + 3T_{1u} + 3T_{2u} + 2E_u + 3T_{1u} + 1A_{2u}$. T_{1u} modes are IR active, while the modes with T_{2g} symmetry have Raman active vibrations. The two E_u and one A_{2u} modes are silent. Although the electronic structure of Mg_2La is strongly metallic with high density of states at Fermi level, the large splitting of transverse and longitudinal optical modes at Γ-point is an indication of partial ionicity of crystal bonding mechanism.

4. Conclusion

In this study, we present the ab initio density functional calculations results of elastic and vibrational properties of Mg_2La cubic Laves structure. The elastic properties have been studied up to 150 GPa pressure. The studied phase remains stable within this pressure range. The system seems to show an electronic topological transition around 100 GPa as revealed by elastic anisotropy ratio and electronic bands. The three selected electronic bands pass through Fermi level with increasing pressure. This picture indicates the sensitivity of elastic properties to Fermi surface structure. The material becomes more ductile under compression. The phonon spectra do not show any vibrational anomaly to verify the stability of cubic phase.

Acknowledgements

This research was supported in part by TÜBİTAK (The Scientific & Technological Research Council of Turkey) through TR-Grid e-Infrastructure Project, part of the calculations have been carried out at ULAKBİM Computer Center.

References

[1] Y. Ouyang, X. Tao, H. Chen, Y. Feng, Y. Du, Y. Liu, Comput. Mater. Sci. 47 (2009) 297.
[2] Y. Wu, W. Hu, Eur. Phys. J. B 60 (2007) 75.
[3] N. Fujita, S. Kikuchi, A.P. Tsai, Solid state Sci. 13 (2011) 698.
[4] W.Y. Yu, N. Wang, X.B. Xiao, B.Y. Tang, L.M. Peng, W.J. Ding, Solid State Sci. 11 (2009) 1400.
[5] P. Aroule, IMA-55, A Global Vision for Magnesium, International Magnesium Association, Washington, DC, 1998, pp. 36–46.
[6] C. Cazorla, D. Errandonea, E. Sola, Phys. Rev. B 80 (2009) 064105.
[7] F. Stein, M. Palm, G. Sauthoff, Intermetallics 12 (2004) 713.
[8] F. Laves, H. Witte, Metall-Wirtschaff Wiss Tech. 14 (1935) 645.
[9] K.A. Gschneidner Jr., V.K. Pecharsky, Z. Kristallogr. 221 (2006) 375.
[10] P. Paufler, Intermetallics 19 (2011) 599.
[11] J. Wróbel, L.G. Hector Jr., W. Wolf, S.L. Shang, Z.K. Liu, K.J. Kurzydłowski, J. Alloys Compd. 512 (2012) 296.
[12] E.M. Taleff, L.G. Hector Jr., R. Verma, P.E. Krajewski, J.-K. Chang, J. Mater. Eng. Perform. 19 (2010) 488.
[13] J.A. Yasi, L.G. Hector Jr., D.R. Trinkle, Acta Mater. 58 (2010) 5704.
[14] B.L. Mordike, T. Ebert, Mater. Sci. Eng. A 37 (2001) 302.
[15] Y.F. Wang, W.B. Zhang, Z.Z. Wang, Y.H. Deng, N. Yu, B.Y. Tang, X.Q. Zeng, W.J. Ding, Comput. Mater. Sci. 41 (2007) 78.
[16] H. Zhang, S. Shang, J.E. Saal, A. Saengdeejing, Y. Wang, L.Q. Chen, Z.K. Liu, Intermetallics 17 (2009) 878.
[17] S. Ganeshan, S.L. Shang, H. Zhang, Y. Wang, M. Mantina, Z.K. Liu, Intermetallics 17 (2009) 313.
[18] X. Tao, Y. Quyang, H. Liu, Y. Feng, Y. Du, Y. He, Z. Jin, J. Alloys Compd. 509 (2011) 6899.
[19] Quantum-ESPRESSO is a community project for high-quality quantum-simulation software, based on density-functional theory, and coordinated by Paolo Giannozzi. See http://www.quantum-espresso.org and http://www.pwscf.org.
[20] P. Giannozzi, S. Baroni, N. Bonini, M. Calandra, R. Car, C. Cavazzoni, D. Ceresoli, G.L. Chiarotti, M. Cococcioni, I. Dabo, A. Dal Corso, S. Fabris, G. Fratesi, S. de Gironcoli, R. Gebauer, U. Gerstmann, C. Gougoussis, A. Kokalj, M. Lazzeri, L. Martin-Samos, N. Marzari, F. Mauri, R. Mazzarello, S. Paolini, A. Pasquarello, L. Paulatto, C. Sbraccia, S. Scandolo, G. Sclauzero, A.P. Seitsonen, A. Smogunov, P. Umari, R.M. Wentzcovitch, J. Phys.: Condens. Matter 21 (2009) 395502.
[21] J.P. Perdew, K. Burke, M. Ernzerhof, Phys. Rev. Lett. 77 (1996) 3865.
[22] N.A.W. Holzwarth, A.R. Tackett, G.E. Matthews, Comput. Phys. Commun. 135 (2001) 329.
[23] A.M. Rappe, K.M. Rabe, E. Kaxiras, J.D. Joannopoulos, Phys. Rev. B 41 (1990) 1227.
[24] D. Vanderbilt, Phys. Rev. B 41 (1990) 7892.
[25] G. Kresse, D. Joubert, Phys. Rev. B 59 (1999) 1758.
[26] H.J. Monkhorst, J.D. Pack, Phys. Rev. B 13 (1976) 5188.
[27] N. Marzari, D. Vanderbilt, A.D. Vita, M.C. Payne, Phys. Rev. Lett. 82 (1999) 3296.
[28] G. Steinle-Neumann, L. Stixrude, R.E. Cohen, Phys. Rev. B 60 (1999) 791.
[29] O. Gülseren, R.E. Cohen, Phys. Rev. B 65 (2002) 064103.
[30] G. Gökoğlu, A. Erkişi, Solid State Commun. 147 (2008) 221.
[31] G. Gökoğlu, J. Alloys Compd. 478 (2009) 653.
[32] P. Vinet, J. Ferrante, J.R. Smith, J.H. Rose, J. Phys. C 19 (1986) L467.
[33] X. Gonze, Phys. Rev. A 52 (1995) 1086.
[34] X. Gonze, Phys. Rev. A 52 (1995) 1096.
[35] S. Baroni, S. de Gironcoli, A.D. Corso, Rev. Mod. Phys. 73 (2001) 515.
[36] J.C. Slater, J. Phys. Chem. 41 (1964) 3199.
[37] P. Villars, L.D. Calvert, Pearson's Handbook of Crystallographic Data for Intermetallic Phases, vols. 1–4, ASM International, Materials Park, OH, USA), 1991.
[38] H.B. Schlegel, J. Comput. Chem. 3 (1982) 214.
[39] I.M. Lifshitz, Sov. Phys. JETP 11 (1960) 1130.
[40] L. Dagens, J. Phys. F 8 (1978) 2093.
[41] B.K. Godwal, A. Jayaraman, S. Meenakshi, R.S. Rao, S.K. Sikka, V. Vijayakumar, Phys. Rev. B 57 (1999) 773.
[42] S.F. Pugh, Philos. Mag. 45 (1954) 823.
[43] D.G. Pettifor, Mater. Sci. Technol. 8 (1992) 345.
[44] K. Chen, L.R. Zhao, J. Rodgers, J.S. Tse, J. Phys. D: Appl. Phys. 35 (2003) 2725.